Journal of Oceanology and Limnology
Vol. 36 No. 3, P. 687-699, 2018
https://doi.org/10.1007/s00343-018-7026-8

Control of subduction rate on Tonga-Kermadec arc magmatism*

LUO Qing (罗青)[1, 2], ZHANG Guoliang (张国良)[1, 3, 4, **]

[1] *Key Laboratory of Marine Geology and Environment, Institute of Oceanology, Chinese Academy of Sciences, Qingdao 266071, China*

[2] *University of Chinese Academy of Sciences, Beijing 100049, China*

[3] *Laboratory of Marine Geology, Qingdao National Laboratory for Marine Science and Technology, Qingdao 266071, China*

[4] *Deep-Sea Extreme Environment and Life Processes Center, Institute of Oceanology, Chinese Academy of Sciences, Qingdao 266071, China*

Received Jan. 20, 2017; accepted in principle Apr. 17, 2017; accepted for publication May 16, 2017

Abstract Dehydration/melting of oceanic crusts during returning to the mantle in subduction zones are related to origin of arc lavas. The factors that influence arc magmatism include compositions of the subducting slabs, mantle wedge and subduction rates. However, distinguishing these factors remains difficult and highly debated. Subducting rate is related to the total mass of inputs and controls thermal structure, thus plays a crucial role in arc magmatism. Here we explore the relationships between geochemical variations of arc lavas and convergence rates (increasing from 46 mm/a to the south to 83 mm/a to the northward) in the Tonga-Kermadec arc system. Data of geochemistry for lava samples from nine islands of this arc system are collected and compiled to investigate the role of subduction rate in arc magmatism. Lavas from the northern Tonga arc with a faster subduction rate show broadly lower concentrations of TiO_2 and high-field-strength elements (HFSEs, e.g. Nb, Ta, Zr, Hf), and higher Ba/Th, U/Th ratios than the Kermadec Arc to the south. Some of the Kermadec lavas show the highest values of Th/Nb ratio. We suggest that the northern Tonga arc with a higher subduction rate has been influenced by a stronger role of subduction-released fluid, which results in stronger large-ion-lithophile elements (LILEs) and relatively weaker HFSEs contribution. It is interpreted that faster subduction rate tend to create a cooler subduction zone, leading to stronger dehydration subduction slab contribution with, thus, higher LILE/HFSE ratios of arc lavas. The conclusion contributes to a better understanding of arc magmatism, and ultimately the long-term chemical differentiation of the Earth. More supplementary geochemical data along Tonga-Kermadec arc and tests in other arcs are needed.

Keyword: subduction rate; arc magmatism; Tonga-Kermadec Arc

1 INTRODUCTION

The arc system is an active plate boundary where subduction-related magmatism occurs. However, the factors that control arc magmatism are still highly debated due in part to the complexity of convergent plates (Hawkesworth et al., 1993; Pearce and Peate, 1995; Stern, 2002; Elliott, 2003; Evans, 2012; Spandler and Pirard, 2013). Geochemical studies demonstrated distinct LILEs enrichment and HFSEs depletion in island arc lavas from the mid-ocean ridge basalts (MORBs). Addition of aqueous fluids/melt derived from subducting plates is considered to be responsible for these geochemical signatures (Johnson and Plank, 1999; Elliott, 2003). Other contributions, e.g. variably depleted mantle wedge melt and locally subducted seamounts or hotspots nearby, are also suggested to affect arc lavas (Turner et al., 2009;

* Supported by the National Natural Science Foundation of China (Nos. 41376065, 41522602), the National Program on Global Change and Air-Sea Interaction (No. GASI-GEOGE-02), the Strategic Priority Research Program of Chinese Academy of Sciences (No. XDA11030103), and the Project of "AoShan" Excellent Scholar for Qingdao National Laboratory for Marine Science and Technology
** Corresponding author: zhangguoliang@qdio.ac.cn

Timm et al., 2013; Price et al., 2016). Meanwhile, approaches on geophysical observations and computational models help to constrain the geometry and physical conditions of subduction process. Of particular essential is the thermal structure of subduction zones, which dominates the conditions for the generation of slab-derived fluids and arc volcanism (van Keken et al., 2002; Syracuse et al., 2010; van Keken et al., 2011). A wide range of physical parameters have been identified to influence the temperature distributions, including the age of the incoming lithosphere, shear heating, dig angle, and subduction rate (Peacock, 1990a, 1996; Zellmer et al., 2015). England and Katz, 2010 established a calculation formula to discriminate the scaling relations between these parameters and the temperature field within subduction zone.

Building a linkage between the various approaches is needed, because the degree and depth of dehydration of the subduction plates strongly dependent on the thermal structure of subduction zones (van Keken et al., 2011), thereby influence the melt productivity (Kelley et al., 2006) and arc magmatism. In this paper, we focus in particular on the role of the most obviously varying parameter, subduction rate, which increase from the south (~46 mm/a) to north (~83 mm/a) (Bevis et al., 1995), and explore the geochemical reflection of subduction rate in Tonga-Kermadec arc lavas.

2 GEOLOGICAL SETTING AND DATA SOURCE

The Tonga-Kermadec trench extends nearly linearly NNE from the north of New Zealand to the northern end of the Tongan Islands for some 2 800 km, delineates the collision zone between the Pacific and Indo-Australia plates (Fig.1). A series of ridges and basins, including the Tonga-Kermadec ridge (frontal arc), the Lau-Havre trough (interarc basin), and the Lau-Colville ridge (third arc), are located to the west of the trench. The Louisville seamount chain intersects with the arc at 25°S, which constitutes the boundary between the Tonga (north) and Kermadec (south) arcs. A dozen of islands are distributed along the Tonga-Kermadec ridge, of which major islands from north to south include, e.g., Fonualei, Tofua, Hunga Ha'apai, Ata, Raoul Island Group, Macauley, and Healy. On the Kermadec ridge there are also a number of underwater volcanos, e.g., Monowai, Healy, Rumble Group.

The subduction of the Pacific plate downward to the Australian plate started after the early Eocene. The convergence rates vary linearly with latitude from 83 mm/a to the north of Tonga, which is a global maximum, to 46 mm/a at the south end of the Kermadec trench (Demets et al., 1990; Bevis et al., 1995). The dip of subduction zone changes from approximately 43°–45° beneath Tonga arc to 55°–60° beneath Kermadec arc (Pelletier and Louat, 1989). The age of the Pacific plate respectively increases from ~86 to 125 Ma north and south of the Osbourn trough, a paleo-spreading center (Sutherland and Hollis, 2001; Zhang and Li, 2016). The geochemical analyses of basalt samples drilled at IODP Site U1365 (Fig.1) indicate that the subducting oceanic crust mainly consists of low-K tholeiitic N-MORB with significant low temperature alteration features (Zhang et al., 2012; Zhang and Smith-Duque, 2014). The overlying sediment portion decreases in thickness from south (≥500 m at Hikurangi Plateau) to north (~70 m at Site 596), and varies in composition from terrigenous source dominated to mainly pelagic materials (Carter et al., 1996; Plank and Langmuir, 1998). Tuffs and volcaniclastics from Louisville Seamount Chain also contributed to the sediment cover regionally (Regelous et al., 2010).

Lavas erupted from the Tonga arc are dominated by a series of basaltic andesites, with minor andesites and dacites, and sporadically developed felsic dacites. The Kermadec Islands are characterized by low-K tholeiitic basalts, basaltic andesites, dacites, and low-K rhyolites. Felsic pumiceous clasts occur in pyroclastic flow and deposits on Kermadec Islands (Falloon et al., 1987; Ewart et al., 1994, 1998; Smith and Price, 2006). Moreover, boninites appear at a volcano ~30 km near the Tonga arc island group of Hunga Ha'apai and the northernmost of Tongan ridge (Falloon and Crawford, 1991; Falloon et al., 2008; Cooper et al., 2010).

Tonga-Kermadec arc lavas have been extensively studied in the past few decades. Multiple components have been identified by previous geochemical investigations. The Tonga-Kermadec arc magma source is believed to be generated from the partial melting of the underlying mantle wedge, which is suggested to be increasingly depleted northward due to prior melt extraction in the back-arc (Woodhead et al., 1993; Ewart et al., 1998; Caulfield et al., 2008). Superimposed on the mantle wedge source is the aqueous fluid derived from the subducting Pacific plate by dehydration, which has been identified by high LILE/HFSE ratios (Turner and Hawkesworth, 1997; Ewart et al., 1998). These fluid signatures are

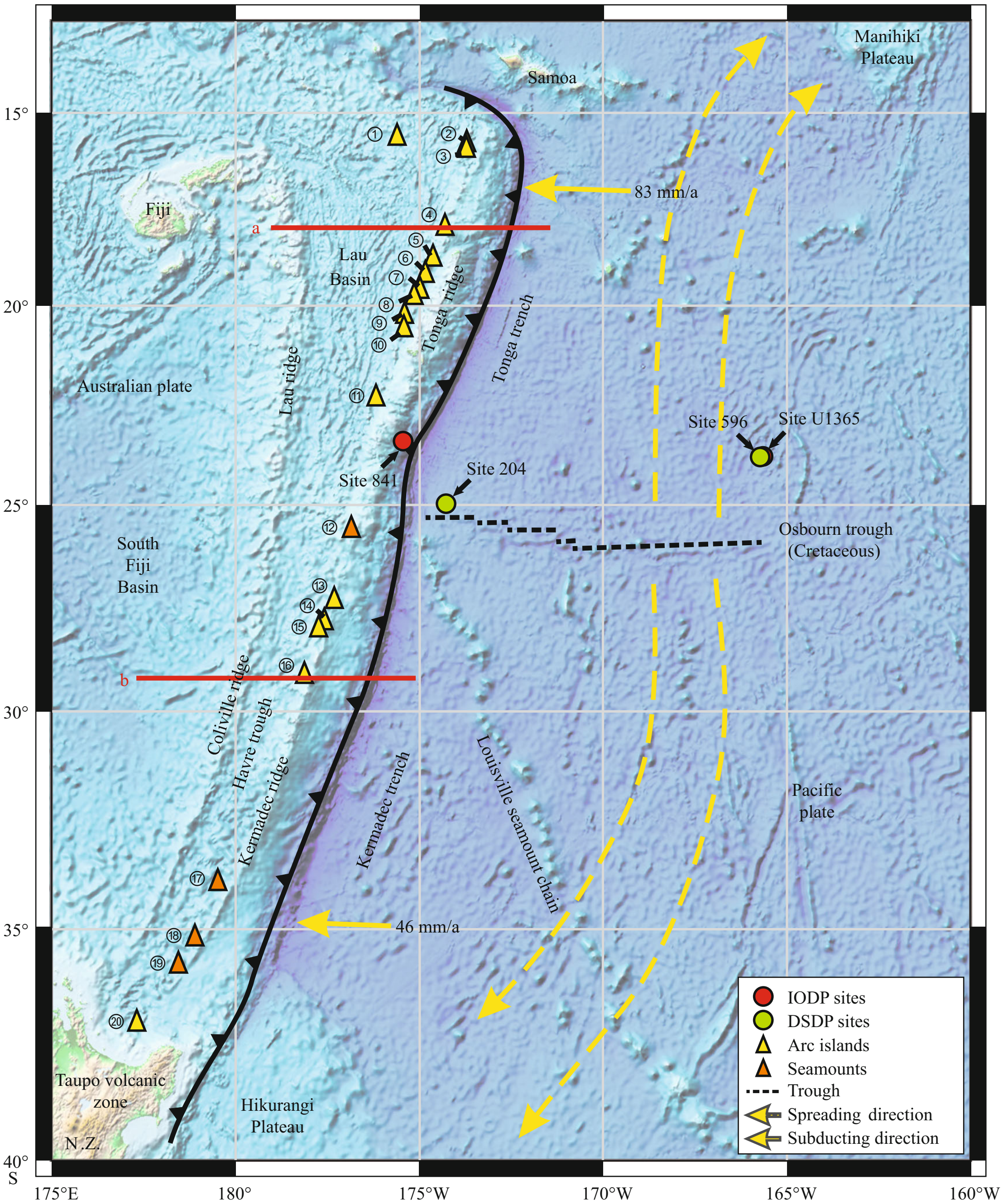

Fig.1 Locality map and sketch showing the topography and tectonic setting of the Tonga-Kermadec subduction zone

The islands in the map are: 1. Niua fo'ou; 2. Tafahi; 3. Niuatoputatu; 4. Fonualei; 5. Late; 6. Metis Shoal; 7. Kao; 8. Tofua; 9. Falcon; 10. Hunga Ha'apai; 11. Ata; 12. Monowai Seamount; 13. Raoul; 14. Macauley; 15. Curtis; 16. L'Esperance; 17. Healy; 18. Rumble III; 19. Rumble IV; 20. Ngatoro Ridge. The bathymetric and elevation data are from NOAA (http://www.ngdc.noaa.gov/mgg/bathymetry/relief.html).

noted to decrease southward along the arc, although they do not occur systematically from island to island. The geochemical tends were interpreted by the variations of component and amount of subducted materials (Regelous et al., 1997; Turner et al., 1997; Ewart et al., 1998; Castillo et al., 2009). Minor contributions of subducted local geochemical anomalies, e.g. seamounts, plateaus, and regional dominated terrigenous sources, were also added to the source of the arc lavas. Lavas from Tafahi and Niuatoputapu Islands on the northern edge of Tonga arc show evidences of either the influence of OIB-material from the Louisville Seamount Chain, or the plume-type mantle from Samoa plateau for their distinct high concentrations of Nb relative to other HFSEs (Wendt et al., 1997; Ewart et al., 1998; Tian et

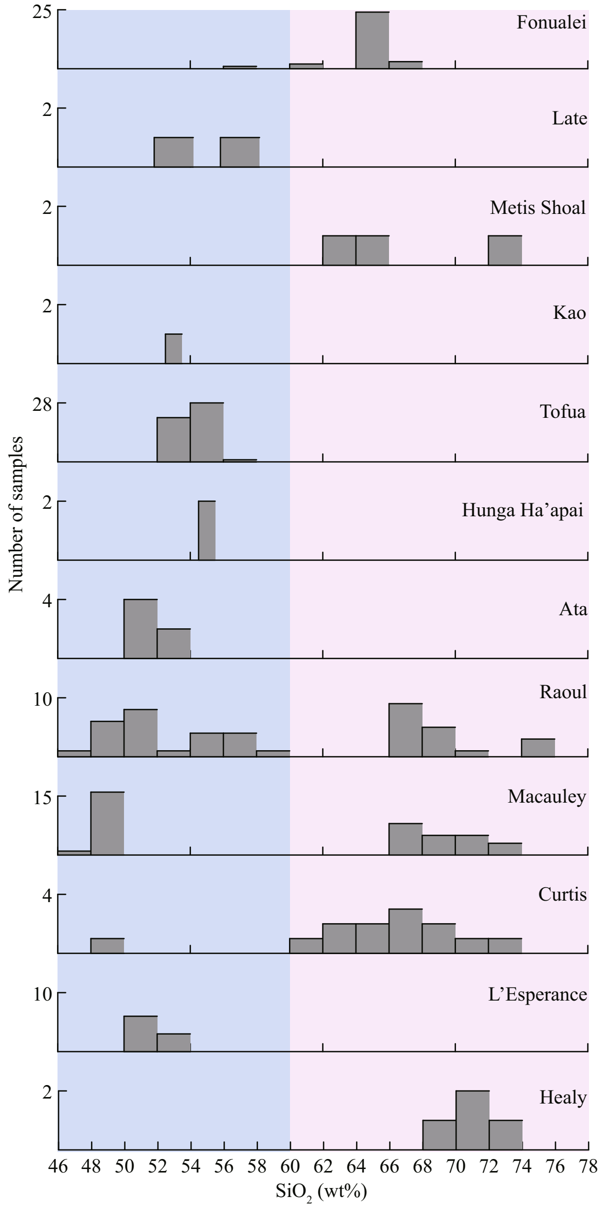

Fig.2 Histograms of SiO_2 (wt%) content in samples of the Tonga-Kermadec lavas

al., 2011; Haase et al., 2016). The more radiogenic Pb isotopes in lavas from volcanoes of southern Kermadec arc, including Rumble series, and Ngatoro ridge, reflect the addition of terrigenous sediments supplied by New Zealand (Ewart et al., 1998), and perhaps the subduction of Hikurangi Plateau (Timm et al., 2014, 2016). The influences of Louisville seamounts also occur in Monowai lavas evidenced by higher $^{206}Pb/^{204}Pb$ (Timm et al., 2011).

The major and trace element data used in this paper are collected from previously published studies (Ewart and Hawkesworth, 1987; Gamble et al., 1996; Turner et al., 1997, 2000, 2012; Ewart et al., 1998; Clift et al., 2001; Barker et al., 2013), and the samples used were collected from young volcanic eruptions (<10 Ma). To exclude the influences from the adjacent plateaus and the subduction of seamounts, we eliminated data from Islands of Niua fo'ou, Tafahi, Niuatoputapu at the northernmost of Tonga Arc, and Rumble III, Rumble IV and Ngatoro Ridge at the southernmost of Kermadec arc. We treat Tonga and Kermadec arcs as two separate populations and analyze the data as two groups.

A histogram of the collected lava data from Tonga-Kermadec Islands shows that, the SiO_2 content forms a bimodal distribution consisting of two sub-populations and very few samples in the range of 58%–62%, which is previously observed by Smith et al., 2006 (Fig.2). The lavas with SiO_2 content >60% have been suggested to reflect the mixing of a silicic melt component potentially generated from subducted crust melting (Smith et al., 2010). Therefore, we selected samples with SiO_2 content <60% to better represent mantle-derived arc lavas source.

On primitive mantle normalized diagrams (Fig.3), lavas from both Tongan and Kermadec Islands have typical features of LILEs enrichment and HFSEs depletion. Although Tongan and Kermadec samples have similar REEs patterns, integral differences do exist between the two segments. Kermadec samples show larger ranges of rare earth element (REEs) concentrations (Fig.3a), while Tongan samples have lower averaged REEs concentrations (Fig.3b). Moreover, Tongan lavas have obviously higher averaged concentrations of fluid mobile elements (e.g. Cs, Rb, Ba, U, K, Pb and Sr) and stronger depletion of incompatible fluid immobile elements (e.g. Nb, Ta, Zr, Hf and heavy REEs).

Differences between Tongan and Kermadec lavas are best illustrated by the ratios Ba/Th, U/Th, and Th/Nb (Fig.4). The Tonga segment shows significant greater values of Ba/Th and U/Th ratios than that of Kermadec, although the averaged values do not increase from south to north continually. The values of Ce/Pb ratio in Tonga lavas are slightly lower than that of Kermadec. Tofua on the Tonga arc show the greatest range and highest values of Ba/Th and U/Th, while L'Esperance seamount at the southernmost of Kermadec segment appear to have the highest values of Th/Nb. The only exception is the Ata Island, which has lavas with lower Ba/Th, U/Th, and higher Ce/Pb, Th/Nb values than most other lavas from both segments.

Similar differentiations occur in TiO_2 concentrations.

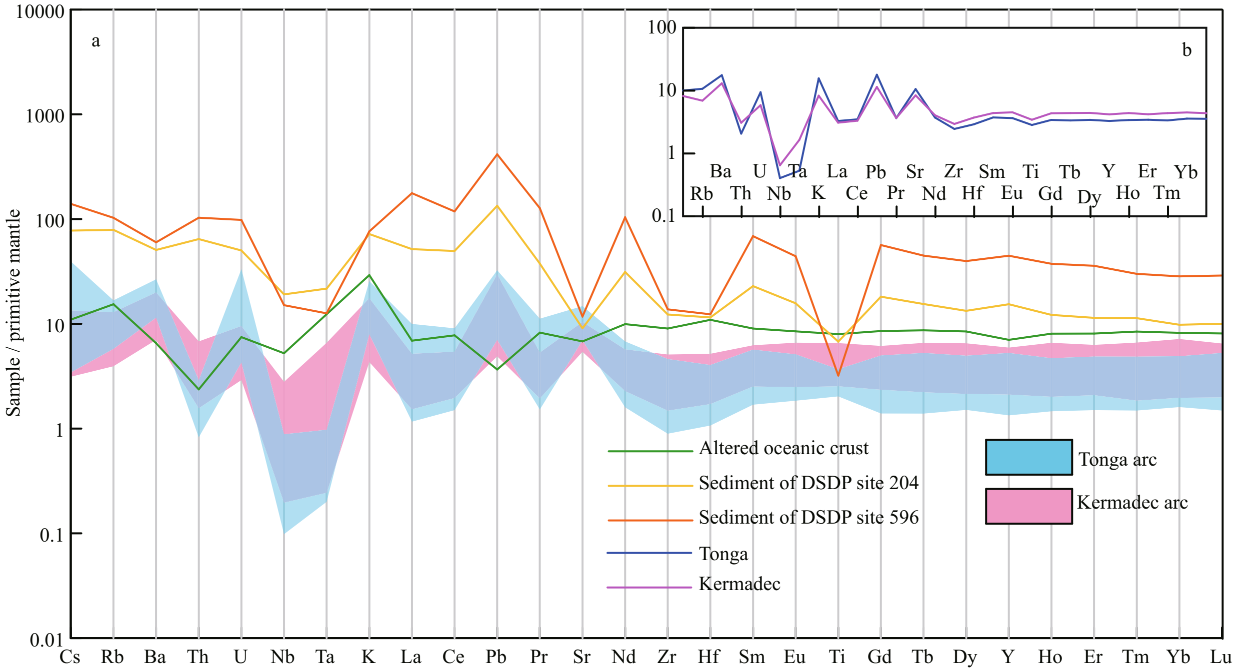

Fig.3 Patterns of primitive mantle normalized REEs and incompatible elements (a) and averaged REEs (b)

Colored blocks show the ranges of data, colored lines represent averaged data. Data of sediments of Site 596 and Site 204 are from Ewart et al., 1998. Data of altered oceanic crust are from Zhang and Smith-Duque, 2014. Data of Indian MORBs and Pacific MORBs for comparison are from PetDB database (http://www.earthchem.org/petdb). Data of primitive mantle for normalization are from McDonough and Sun, 1995.

For Fig.5a, the lavas of Kermadec segment show relatively greater range of TiO_2 and MgO, and higher TiO_2 concentrations for a given MgO content than lavas of the Tonga arc. When potted versus Ba/Th ratio, TiO_2 concentrations appear to be negative correlated. Samples of Tofua at Tonga arc with higher Ba/Th ratios tend to show lower TiO_2 values.

3 DISCUSSION

3.1 Form of subduction addition

Before we discuss the influences of thermal structures on arc lavas, it is crucial to figure out the forms of contribution of subduction materials, because the dehydration or melting of mineral phases are significantly constrained by temperature.

This issue has been previously investigated by abundant studies. Two chemically distinct components are defined to be derived from the subducting slab in arc lavas records. The first is a sediment delivered partial melt, which contributes a range of incompatible elements to the mantle wedge and is responsible for the enrichment of most REEs (Elliott et al., 1997; van Keken et al., 2002). The second is an aqueous fluid, which selectively transport the highly fluid-mobile elements (e.g. Rb, Ba, Pb), and is suggested to be delivered mainly from the altered oceanic crust rather than sediment (Morris et al., 1990; Clift et al., 2001), or from all available components (Hoogewerff et al., 1997; Haase et al., 2002). ^{10}Be is a cosmogenic radioisotope that is highly enriched in marine sediments. High $^{10}Be/^{9}Be$ in arc lavas is treated as conclusive evidence for the addition of subducted sediments into arc magma sources (e.g., Morris et al., 1990). For Tonga-Kermadec Arc, pelagic sediment contribution has been recognized by more recent ^{10}Be isotope data (George et al., 2005), and fluid addition were inferred to be delivered from slab dehydration by the record of U-Th isotope disequilibrium (Turner et al., 1997).

As explained by Pearce et al., 2005, Ratios of elements of similar incompatibilities, one mobile and one immobile, are useful to constrain subduction inputs. Experiments show that Ba and U are significantly partitioned into aqueous fluids derived from the subduction slab, while both Ba, U and Th are significantly partitioned into siliceous melts (Plank and Langmuir, 1993; Keppler, 1996; Johnson and Plank, 1999; Plank, 2005). In contrast, Nb is relatively immobile unless a rutile-bearing slab melts at the highest temperature (Brenan et al., 1994). Consequently, high Ba/Th and U/Th indicate the lower-temperature fluid addition, as both elements are mobilized in melts but only Ba and U are mobilized in fluids. In contrast, Th enrichment, and hence high Th/Nb, indicates the higher temperature melt component

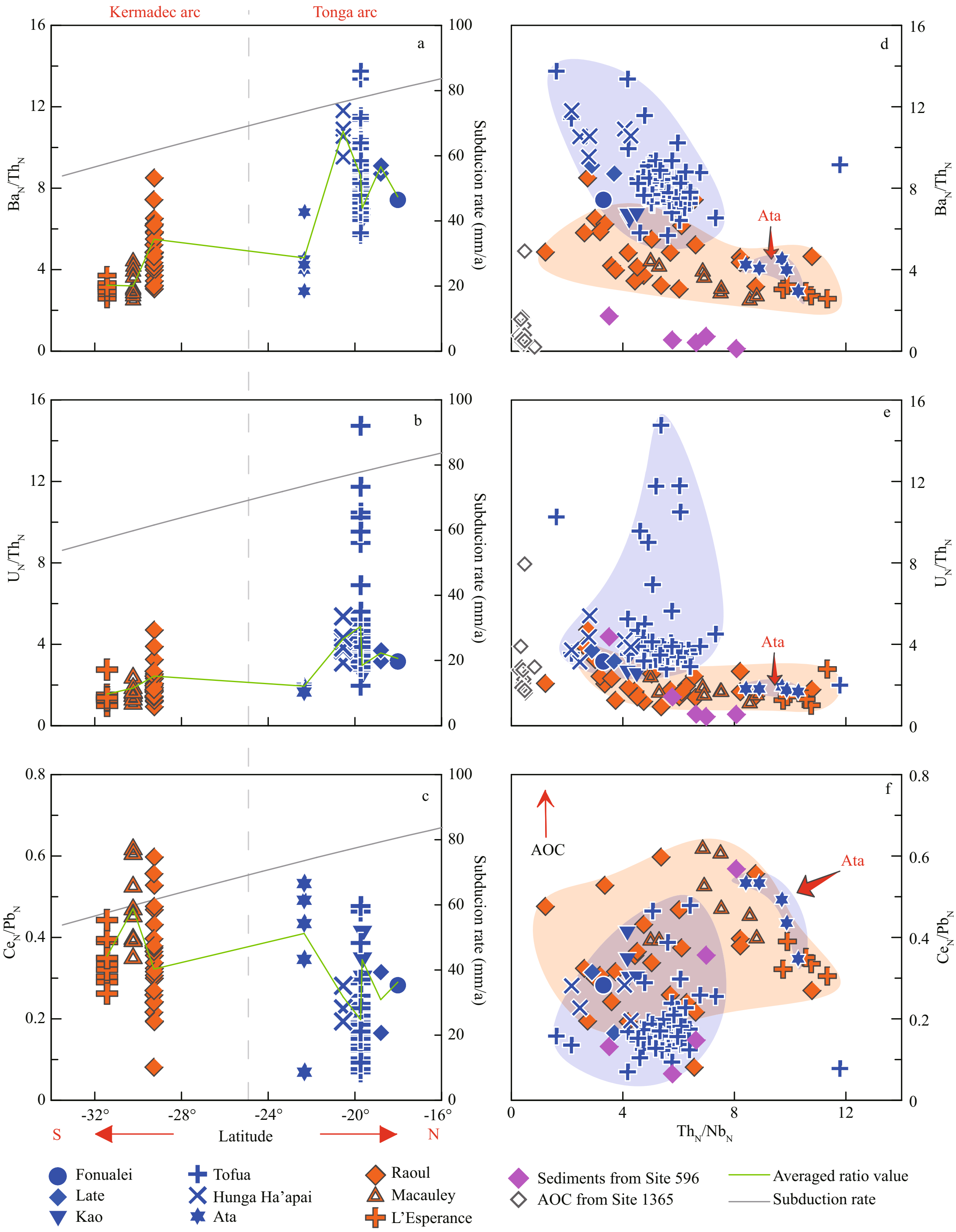

Fig.4 Plots showing primitive mantle normalized ratios of Ba/Th, U/Th, Ce/Pb, and subduction rate vs. latitude (a–c) and Th/Nb (e–f)

Data of subduction rate are from Plate Motion Calculator (http://www.unavco.org/software/geodetic-utilities/plate-motion-calculator/plate-motion-calculator.html), using Australia Plate as reference.

(probably sediment melt, as suggested by Elliott et al., 1997).

For Fig.4d–e, samples with higher Ba/Th or U/Th values tend to have lower Th/Nb, implying physically separate sources for Ba and U relative to Th, which support the ideas reviewed above. Except for Ata lavas, which shall be discussed in a later section, Tongan lavas show stronger slab-derived fluid

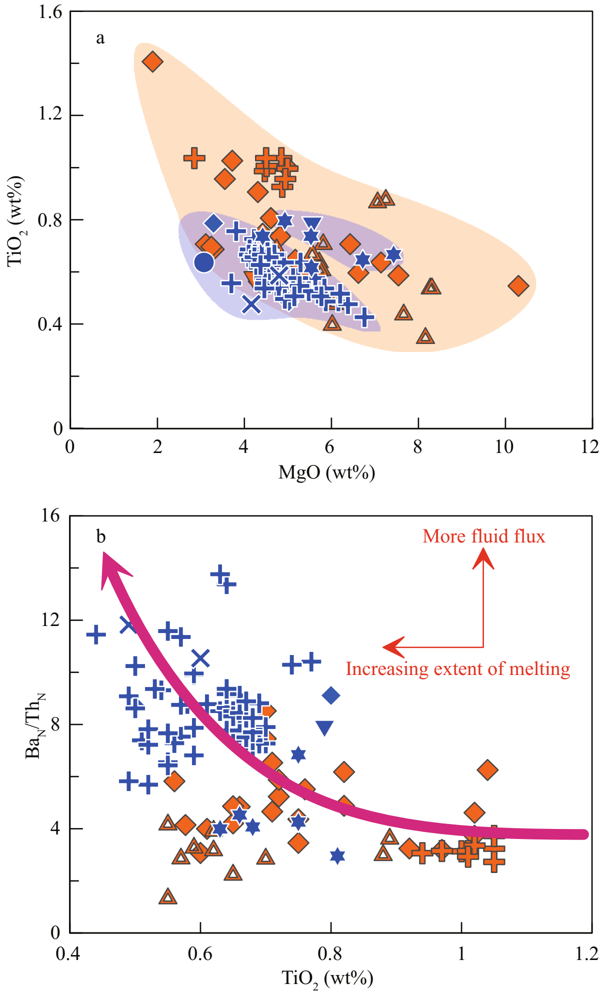

Fig.5 Plots showing TiO_2 (wt%) versus MgO (wt%) (a) and primitive mantle normalized Ba/Th versus TiO_2 (wt%) (b) for Tonga and Kermadec lavas

signature (higher Ba/Th, U/Th). Some of the Kermadec lavas show the highest values of Th/Nb. It is thus indicated that the proportion of slab dehydration is greater under Tongan arc during subduction. The highest values of Th/Nb appear among Kermadec samples represent greater probability of high temperature melting of subduction component.

Pb is considered to be ~10 times more mobile than U during slab dehydration (Kelley et al., 2005), and is preferential enriched in hydrothermal fluids over Ce, therefore Ce/Pb is also a proxy of slab-derived fluids. Most of the subducted Pb is hosted by sulfides in oceanic crust during hydrothermal alteration, and metalliferous deposits in sediments (Peucker-Ehrenbrink et al., 1994; Mühe et al., 1997). In Fig.4f, the slightly lower Ce/Pb of Tonga lavas indicate more Pb addition from subduction materials, also imply stronger slab-derived fluids contribution.

3.2 Volume of subduction input fluxes

The most significant characteristic of Tonga-Kermadec arc system is the gradually increasing rate of plate convergence and back-arc spreading from south to north. Faster subduction rates tend to supply more subducting materials per unit of time. The rate at which bound and free water enters the subduction zone is suggested to be approximately proportional to the convergence rate (Hyndman and Peacock, 2003). Consequently, the relationship of amounts of slab additions and geochemistry of arc lavas needs to be discussed.

Previous studies on mantle melting beneath back-arc basins found that, positive correlations occur between the water concentration of the mantle and the extent of melting (Kelley et al., 2006). Titanium, like other HFSEs, tend to be retained in residual rutile in the slab during dehydration (Ryerson and Watson, 1987). It is thus approximately adopted that, the TiO_2 content of arc magma sources from a given mantle wedge are independent of the slab-derived component. Furthermore, TiO_2 decreases monotonically in the melt with increasing extent of melting of a single source, due to the incompatibility of titanium during mantle melting. Therefore, the variation of TiO_2 concentration in mafic arc lavas is useful to indicate the extent of melting, and shall be correlated with fluid signatures which represent water content of the mantle source.

The TiO_2 values of selected sample data are plotted versus MgO to eliminate the interference of fractional crystallization (Fig.5a). Tongan lavas show lower TiO_2 at given MgO contents. Several studies argued that the low Ti and HFSEs might be generated by depleted mantle wedge reservoir which has been metamorphosed by strong back-arc melt extraction (Ewart et al., 1998). However, the Nb/Ta and La/Sm ratios, which represent mantle wedge depletion (Caulfield et al., 2008), show no obvious distinction between Tonga and Kermadec segments (Fig.6). This contradiction may be interpreted by the southward migration of mantle wedge flow beneath Tonga-Kermadec Arc, as suggested by Turner and Hawkesworth, 1998. The diagram of Ba/Th versus TiO_2 shows negative correlation (Fig.5b), which means greater fluid contributions tend to stimulate higher extent of partial melting in mantle wedge. It is indicated that (1) larger amount of subducted slab driven by faster subduction rates entered Tonga trench and contributed to the arc lavas, leading to stronger fluid signatures; (2) the lower HFSE concentrations in Tongan lavas are resulted from greater extents of melting rather than prior depletion of the source.

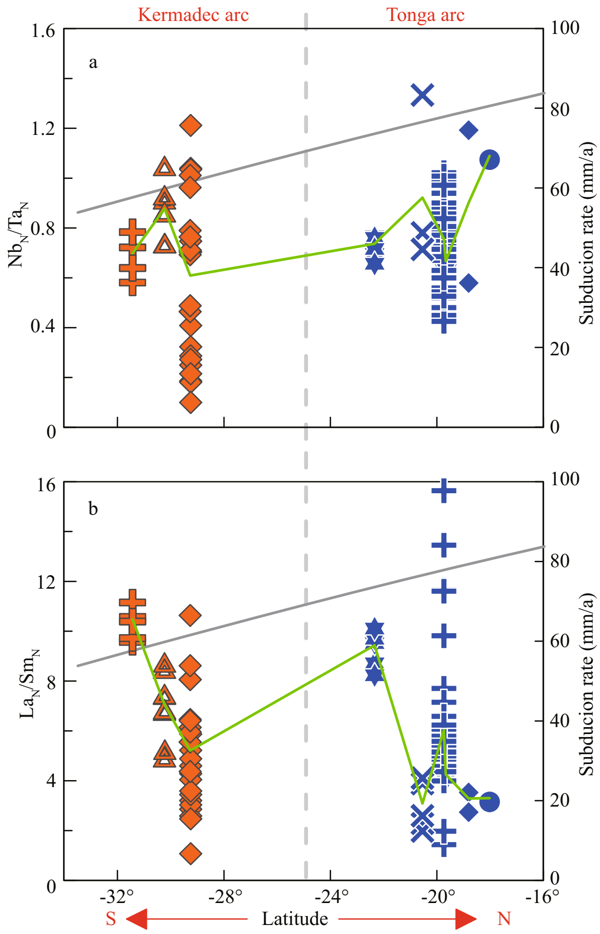

Fig.6 Plots showing primitive mantle normalized ratios of Nb/Ta, La/Sm and subduction rate vs. latitude (a, b) and MgO (wt%) (c, d)

3.3 Thermal structure

The thermal structure of subduction zones has been of intriguing interest for a long time. Plenty of reasonable predictions have been achieved particularly from geochemical observations and numerical simulations. Syracuse et al. (2010) calculated the thermal model of Tonga and Kermadec arc segments under different partial coupling causes, obtained lower slab and Moho temperature, and higher maximum mantle temperature at deeper depth in Tonga segment beneath arc. This consequence is an important reference for the following discussion.

The highest values of Th/Nb ratios of Kermadec lavas represent greatest high temperature sediment melt addition. Turner et al. (1997) and Ewart et al. (1998) recognized the variation tendency of more radiogenic Pb isotope compositions and higher Th/U ratios in Kermadec lavas, and attributed it to the thicker sediment to the south. Indeed, the thickness of sediment entering the Tonga-Kermadec trench show increasing trend southward, which changes from ~150–300 m (Crawford et al., 2003) to <200 m around Louisville Seamounts (Contreras-Reyes et al., 2011) and to ≥500 m at Hikurangi Plateau (Carter et al., 1996). However, there is no accurate continual measurement of sediment thickness from south to north. We thus make an assumption that sediment thickness varies continually and linearly. From Tofua to L'Esperance Island, the thickness of the subducted sediment may be 200 m to 250 m. As concluded in the last section, faster subduction rate shall introduce lager amount of subducting materials into mantle wedge sources. The calculated sediment fluxes per unit time for the two segments are almost the same. Therefore, the greater sediment signature in Kermadec lavas is better interpreted by warmer thermal structure, which lead to more sediment melt added to arc magma reservoir. This is consistent with the simulated results mentioned above.

An adminiculary evidence for the dominant role of thermal structure is the geochemical exception of Ata lavas. The Ata Island, located at the junction of Tonga and Kermadec segment, was expected to represent intermediate geochemical characteristics between slab dehydration characterized composition in the north and sediment melting characterized composition in the south. However, Ata lavas show high values of Th/Nb, low values of Ba/Th and U/Th similar with those of the Kermadecs, implying abnormal high temperature beneath Ata Island. While at the east of Ata, the adjacent Osbourn Trough, which is interpreted as a fossil spreading center, is subducting westward into the trench. The subduction of spreading center was suggested to generate extraordinary hot subduction zones (Hibbard et al., 1993; Peacock, 1996). What's more, in the model of Kirby et al. (1991), the slab temperature also depends on slab age, whereas older lithosphere may cool the mantle wedge more efficiently. Therefore, the geochemical anomalies of Ata lavas may be inferred as the result of Osbourn Trough or young hotter slab subduction, which lead to a thermal structure hot enough to induce sediment partial melting, similar to the consequences of slower subduction rates at south Kermadec.

The thermal structure of subduction zone could be affected by many factors, i.e. convergence rate, slab dip, slab age, and mantle thermal diffusivity (Kirby et al., 1991; England and Katz, 2010). There are different opinions on the thermal impacts of convergence rate. Someone suggested faster subduction rates tend to produce cooler subduction zones through introducing

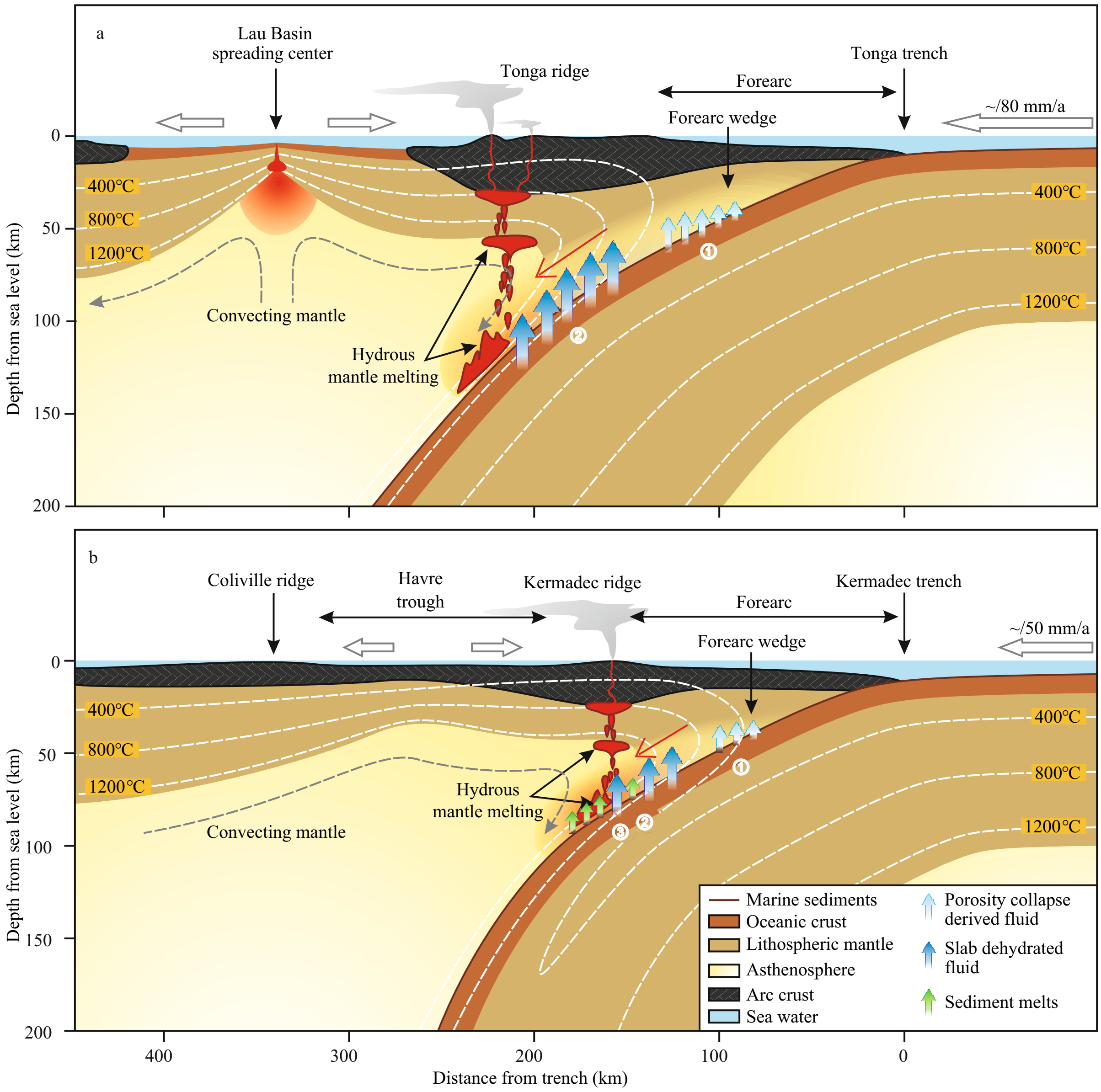

Fig.7 Schematic cross-section diagram illustrating the different subduction processes occurring beneath the Tonga (a) and Kermadec (b) subduction zones

The position of the two sections are marked on Fig.1. The subduction process is divided into three phases: (1) free water and fluids are derived from subduction slabs through sediment densification and porosity collapse at shallow depths (10–30 km) near the trench, and generally serpentinize the cold mantle wedge under forearcs (Hyndman and Peacock, 2003); (2) the slab sinks to a proper depth, with the increasing of temperature and pressure, large amounts of fluids are released by continuous dehydration reactions that occur in subducting oceanic crust during pressure-dependent amphibolite → eclogite facies metamorphism (Hyndman and Peacock, 2003; Grove et al., 2009). These fluids infiltrate and hydrate the upper mantle wedge, generate hornblende peridotite. The LILEs are stored in the crystal lattices of hydrous minerals like amphiboles and phlogopites. This dehydration area may extend to 60–80 km at cold subduction zones; (3) the hydrated mantle are dragged downward (red arrows) with convection in the wedge until it crosses the solidus of amphibole peridotite (~1 000°C, 70–100 km) and undergoes partial melting (Green, 1973; Wyllie, 1979). Sediments are suggested to melt and contribute to the arc lava source region at this depth (Turner and Hawkesworth, 1997).

cold slabs (Peacock, 1990b). Others hold the idea that faster subduction rates may warm the subduction zones by inducing stronger corner flow (Conder and Wiens, 2007), hence more heat from the wedge is drawn to the slab interface (van Keken et al., 2002). However, for Tonga-Kermadec arc system, faster subduction rate is correlated to cooler thermal structure and less sediment-derived melt, which indicate a dominant role of the cooling effect of cold subduction slabs.

3.4 Modified subduction models

Based on the discussions above, we propose a modified contrast model for the Tonga and Kermadec arc segments (Fig.7).

In Tonga segment, faster subduction rate introduced more slab into the subduction zone, and descent the temperature of mantle interface. Larger amounts of fluids derived from the slab through dehydration, with high concentrations of fluid-mobile elements (Ba, U, and Pb) were added to the mantle wedge. The more hydrated mantle wedge melt in higher extension, but the temperature was not high enough for massive sediment partial melting. Thus, the Tongan lavas show stronger fluid signatures rather than high-temperature melts.

In contrast, the thermal structure beneath Kermadec segment was less altered by descending slab. The higher temperature allowed subducted sediments to melt more efficiently, and transfer significant amount of Th, which is dominantly supplied by sediments, into the reservoir of arc lavas. Limited amounts of subduction slab entered the subduction zone and contributed less dehydrated fluids into the mantle wedge, thus the fluid signatures (Ba/Th and U/Th)are lower than those of Tonga segment.

4 CONCLUSION

We analyze the major and trace element compositions from the Tonga-Kermadec subduction system, which has an increasing subduction rate from south to north, to investigate the potential effects of subduction rate on arc lava composition. Geochemical differences between the Tonga and Kermadec segments are revealed based on the comparisons of the collected major and trace element data of lavas from 9 islands and underwater volcanoes on the Tonga-Kermadec arc. The Tonga arc lavas are more depleted in HFSEs, with lower TiO_2 content, Ce/Pb ratio, higher Ba/Th and U/Th ratios than those of Kermadec arc. Some of the Kermadec lavas show the highest values of Th/Nb. It is indicated that:

(1) The high Ba/Th and U/Th ratios are mainly attributed to fluid addition derived from slab dehydration, of which the latter dominated by altered oceanic crust. The high Th/Nb ratio component is mainly contributed from subducted sediments by high temperature melts.

(2) The lower TiO_2 content with higher Ba/Th ratio in Tonga lavas indicate a higher extent of melting in the underlying mantle wedge, caused by larger amount of fluid derived from the subducted slab, which is controlled by the subduction rate.

(3) The high values of Th/Nb in Kermadec lavas indicate warmer thermal structures under Kermadec segment, which is less altered by the cold slab.

We suggest that the northward increasing subduction rate is the primary cause to the stronger fluid signatures in northern arc lavas. The contributions from subducted slab are mainly characterized by dehydrated fluids at Tonga arc segment, which have cooler thermal structure due to the faster convergence rate, and by sediment partial melts at Kermadec segment with slower convergence rate.

5 DATA AVAILABILITY STATEMENT

The data analyzed during the current study are cited from these published article (Ewart and Hawkesworth, 1987; Gamble et al., 1996; Turner et al., 1997, 2000, 2012; Ewart et al., 1998; Clift et al., 2001; Barker et al., 2013) and the following public repository: http://www.earthchem.org/petdb.

References

Barker S J, Wilson C J N, Baker J A et al. 2013. Geochemistry and petrogenesis of silicic magmas in the intra-oceanic Kermadec arc. *Journal of Petrology*, **54**(2): 351-391, https://doi.org/10.1093/petrology/egs071.

Bevis M, Taylor F W, Schutz B E et al. 1995. Geodetic observations of very rapid convergence and back-arc extension at the Tonga arc. *Nature*, **374**(6519): 249-251, https://doi.org/10.1038/374249a0.

Brenan J M, Shaw H F, Phinney D L et al. 1994. Rutile-aqueous fluid partitioning of Nb, Ta, Hf, Zr, U and Th: implications for high field strength element depletions in island-arc basalts. *Earth and Planetary Science Letters*, **128**(3-4): 327-339, https://doi.org/10.1016/0012-821x(94)90154-6.

Carter L, Carter R M, McCave I N et al. 1996. Regional sediment recycling in the abyssal southwest Pacific Ocean. *Geology*, **24**(8): 735-738, http://geology.gsapubs.org/content/24/8/735.

Castillo P R, Lonsdale P F, Moran C L et al. 2009. Geochemistry of mid-cretaceous pacific crust being subducted along the Tonga-Kermadec trench: implications for the generation of arc lavas. *Lithos*, **112**(1-2): 87-102, https://doi.org/10.1016/j.lithos.2009.03.041.

Caulfield J T, Turner S P, Dosseto A et al. 2008. Source depletion and extent of melting in the Tongan sub-arc mantle. *Earth and Planetary Science Letters*, **273**(3-4): 279-288, https://doi.org/10.1016/j.epsl.2008.06.040.

Clift P D, Rose E F, Shimizu N et al. 2001. Tracing the evolving flux from the subducting plate in the Tonga-Kermadec arc system using boron in volcanic glass. *Geochimica et Cosmochimica Acta*, **65**(19): 3 347-3 364, https://doi.org/10.1016/S0016-7037(01)00670-6.

Conder J A, Wiens D A. 2007. Rapid mantle flow beneath the Tonga volcanic arc. *Earth and Planetary Science Letters*, **264**(1-2): 299-307, https://doi.org/10.1016/j.epsl.2007.10.014.

Contreras-Reyes E, Grevemeyer I, Watts A B et al. 2011. Deep seismic structure of the Tonga subduction zone: implications for mantle hydration, tectonic erosion, and arc magmatism. *Journal of Geophysical Research*, **116**(B10):B10103,https://doi.org/10.1029/2011jb008434.

Cooper L B, Plank T, Arculus R J et al. 2010. High-Ca boninites from the active Tonga arc. *Journal of Geophysical Research*, **115**(B10): B10206, https://doi.org/10.1029/2009JB006367.

Crawford W C, Hildebrand J A, Dorman L M et al. 2003. Tonga ridge and Lau basin crustal structure from seismic refraction data. *Journal of Geophysical Research*, **108**(B4): 2 195, https://doi.org/10.1029/2001JB001435.

Demets C, Gordon R G, Argus D F et al. 1990. Current plate motions. *Geophysical Journal International*, **101**(2): 425-478, https://doi.org/10.1111/j.1365-246X.1990.tb06579.x.

Elliott T, Plank T, Zindler A et al. 1997. Element transport from slab to volcanic front at the Mariana arc. *Journal of Geophysical Research*, **102**(B7): 14 991-15 019, https://doi.org/10.1029/97JB00788.

Elliott T. 2003. Tracers of the slab. *In*: Eiler J ed. Inside the Subduction Factory. Washington, DC: American Geophysical Union. Geophysical Monograph Series, **138**: 23-45.

England P C, Katz R F. 2010. Melting above the anhydrous solidus controls the location of volcanic arcs. *Nature*, **467**(7316): 700-703, https://doi.org/10.1038/nature09417.

Evans K A. 2012. The redox budget of subduction zones. *Earth-Science Reviews*, **113**(1-2): 11-32, https://doi.org/10.1016/j.earscirev.2012.03.003.

Ewart A, Bryan W B, Chappell B W et al. 1994. Regional geochemistry of the Lau-Tonga arc and backarc systems. *Proceedings of the Ocean Drilling Program. Scientific Results*, **135**: 385-425.

Ewart A, Collerson K D, Regelous M et al. 1998. Geochemical evolution within the Tonga-Kermadec—Lau arc—back-arc systems: the role of varying mantle wedge composition in space and time. *Journal of Petrology*, **39**(3): 331-368, https://doi.org/10.1093/petrology/39.3.331.

Ewart A, Hawkesworth C J. 1987. The pleistocene-recent Tonga-Kermadec arc lavas: interpretation of new isotopic and rare earth data in terms of a depleted mantle source model. *Journal of Petrology*, **28**(3): 495-530, https://doi.org/10.1093/petrology/28.3.495.

Falloon T J, Crawford A J. 1991. The petrogenesis of high-calcium boninite lavas dredged from the northern Tonga ridge. *Earth and Planetary Science Letters*, **102**(3-4): 375-394, https://doi.org/10.1016/0012-821x(91)90030-L.

Falloon T J, Danyushevsky L V, Crawford A J et al. 2008. Boninites and adakites from the northern termination of the Tonga trench: implications for adakite petrogenesis. *Journal of Petrology*, **49**(4): 697-715, https://doi.org/10.1093/petrology/egm080.

Falloon T J, Green D H, Crawford A J. 1987. Dredged igneous rocks from the northern termination of the Tofua magmatic arc, Tonga and adjacent Lau basin. *Australian Journal of Earth Sciences*, **34**(4): 487-506, https://doi.org/10.1080/08120098708729428.

Gamble J, Woodhead J, Wright I et al. 1996. Basalt and sediment geochemistry and magma petrogenesis in a transect from oceanic island arc to rifted continental margin arc: the Kermadec-Hikurangi margin, SW Pacific. *Journal of Petrology*, **37**(6): 1 523-1 546, https://doi.org/10.1093/petrology/37.6.1523.

George R, Turner S, Morris J et al. 2005. Pressure–temperature–time paths of sediment recycling beneath the Tonga-Kermadec arc. *Earth and Planetary Science Letters*, **233**(1): 195-211, https://doi.org/10.1016/j.epsl.2005.01. 020.

Green D H. 1973. Experimental melting studies on a model upper mantle composition at high pressure under water-saturated and water-undersaturated conditions. *Earth and Planetary Science Letters*, **19**(1): 37-53, https://doi.org/10.1016/0012-821x(73)90176-3.

Grove T L, Till C B, Lev E et al. 2009. Kinematic variables and water transport control the formation and location of arc volcanoes. *Nature*, **459**(7247): 694-697, https://doi.org/10.1038/nature08044.

Haase K M, Regelous M, Beier C. 2016. Sediment melt flux into the melting zone of the northernmost Tonga island arc. *Mineralogical Magazine*, **75**(3): 962-1 075.

Haase K M, Worthington T J, Stoffers P et al. 2002. Mantle dynamics, element recycling, and magma genesis beneath the Kermadec arc-Havre trough. *Geochemistry*, *Geophysics*, *Geosystems*, **3**(11): 1-22, https://doi.org/10.1029/2002GC000335.

Hawkesworth C J, Gallagher K, Hergt J M et al. 1993. Mantle and slab contributions in ARC magmas. *Annual Review of Earth and Planetary Sciences*, **21**(1): 175-204, https://doi.org/10.1146/annurev.ea.21.050193.001135.

Hibbard J P, Laughland M M, Kang S M et al. 1993. The thermal imprint of spreading ridge subduction on the upper structural levels of an accretionary prism, southwest Japan. *Special Papers*, **273**: 83-102, https://doi.org/10.1130/SPE273-p83.

Hoogewerff J A, Van Bergen M J, Vroon P Z et al. 1997. U-series, Sr-Nd-Pb isotope and trace-element systematics across an active island arc-continent collision zone: implications for element transfer at the slab-wedge interface. *Geochimica et Cosmochimica Acta*, **61**(5): 1 057-1 072, https://doi.org/10.1016/S0016-7037(97)84621-2.

Hyndman R D, Peacock S M. 2003. Serpentinization of the forearc mantle. *Earth and Planetary Science Letters*, **212**(3-4): 417-432, https://doi.org/10.1016/S0012-821x(03)00263-2.

Johnson M C, Plank T. 1999. Dehydration and melting experiments constrain the fate of subducted sediments. *Geochemistry*, *Geophysics*, *Geosystems*, **1**(12): 1 007, https://doi.org/10.1029/1999GC000014.

Kelley K A, Plank T, Farr L et al. 2005. Subduction cycling of U, Th, and Pb. *Earth and Planetary Science Letters*, **234**(3-4): 369-383, https://doi.org/10.1016/j.epsl.2005.03.005.

Kelley K A, Plank T, Grove T L et al. 2006. Mantle melting as a function of water content beneath back-arc basins.

Journal of Geophysical Research, **111**(B9): B09208, https://doi.org/10.1029/2005JB003732.

Keppler H. 1996. Constraints from partitioning experiments on the composition of subduction-zone fluids. *Nature*, **380**(6571): 237-240, https://doi.org/10.1038/380237a0.

Kirby S H, Durham W B, Stern L A. 1991. Mantle phase changes and deep-earthquake faulting in subducting lithosphere. *Science*, **252**(5003): 216-225, https://doi.org/10.1126/science.252.5003.216.

McDonough W F, Sun S S. 1995. The composition of the Earth. *Chemical Geology*, **120**(3): 223-253, https://doi.org/10.1016/0009-2541(94)00140-4.

Morris J D, Leeman W P, Tera F. 1990. The subducted component in island arc lavas: constraints from be isotopes and B-Be systematics. *Nature*, **344**(6261): 31-36, https://doi.org/10.1038/344031a0.

Mühe R, Peucker-Ehrenbrink B, Devey C W et al. 1997. On the redistribution of Pb in the oceanic crust during hydrothermal alteration. *Chemical Geology*, **137**(1-2): 67-77, https://doi.org/10.1016/S0009-2541(96)00151-9.

Peacock S M. 1990a. Numerical simulation of metamorphic pressure-temperature-time paths and fluid production in subducting slabs. *Tectonics*, **9**(5): 1 197-1 211, https://doi.org/10.1029/TC009i005p01197.

Peacock S M. 1990b. Fluid processes in subduction zones. *Science*, **248**(4953): 329-337, https://doi.org/10.1126/science.248.4953.329.

Peacock S M. 1996. Thermal and Petrologic Structure of Subduction Zones. *In*: Gray E B ed. Subduction Top to Bottom. Washington, DC: American Geophysical Union. Geophysical Monograph Series. p.19-113.

Pearce J A, Peate D W. 1995. Tectonic implications of the composition of volcanic arc magmas. *Annual Review of Earth and Planetary Sciences*, **23**(1): 251-285, https://doi.org/10.1146/annurev.ea.23.050195.001343.

Pearce J A, Stern R J, Bloomer S H. 2005. Geochemical mapping of the Mariana arc-basin system: implications for the nature and distribution of subduction components. *Geochemistry*, *Geophysics*, *Geosystems*, **6**(7): Q07006, https://doi.org/10.1029/2004GC000895.

Pelletier B, Louat R. 1989. Seismotectonics and present-day relative plate motions in the Tonga-Lau and Kermadec-Havre region. Tectonophysics, **165**(1-4): 237-250, https://doi.org/10.1016/0040-1951(89)90049-8.

Peucker-Ehrenbrink B, Hofmann A W, Hart S R. 1994. Hydrothermal lead transfer from mantle to continental crust: the role of metalliferous sediments. *Earth and Planetary Science Letters*, **125**(1-4): 129-142, https://doi.org/10.1016/0012-821X(94)90211-9.

Plank T, Langmuir C H. 1993. Tracing trace elements from sediment input to volcanic output at subduction zones. *Nature*, **362**(6422): 739-743, https://doi.org/10.1038/362739a0.

Plank T, Langmuir C H. 1998. The chemical composition of subducting sediment and its consequences for the crust and mantle. *Chemical Geology*, **145**(3-4): 325-394, https://doi.org/10.1016/S0009-2541(97)00150-2.

Plank T. 2005. Constraints from thorium/lanthanum on sediment recycling at subduction zones and the evolution of the continents. *Journal of Petrology*, **46**(5): 921-944, https://doi.org/10.1093/petrology/egi005.

Price A A, Jackson M G, Blichert-Toft J et al. 2016. Geochemical evidence in the northeast Lau basin for subduction of the cook-austral volcanic chain in the Tonga trench. *Geochemistry*, *Geophysics*, *Geosystems*, **17**(5): 1 694-1 724, https://doi.org/10.1002/2015GC006237.

Regelous M, Collerson K D, Ewart A et al. 1997. Trace element transport rates in subduction zones: evidence from Th, Sr and Pb isotope data for Tonga-Kermadec arc lavas. *Earth and Planetary Science Letters*, **150**(3-4): 291-302, https://doi.org/10.1016/S0012-821x(97)00107-6.

Regelous M, Gamble J A, Turner S P. 2010. Mechanism and timing of Pb transport from subducted oceanic crust and sediment to the mantle source of arc lavas. *Chemical Geology*, **273**(1-2): 46-54, https://doi.org/10.1016/j.chemgeo.2010.02.011.

Ryerson F J, Watson E B. 1987. Rutile saturation in magmas: implications for Ti-Nb-Ta depletion in island-arc basalts. *Earth and Planetary Science Letters*, **86**(2-4): 225-239, https://doi.org/10.1016/0012-821x(87)90223-8.

Smith I E M, Price R C. 2006. The Tonga-Kermadec arc and Havre-Lau back-arc system: their role in the development of tectonic and magmatic models for the western pacific. *Journal of volcanology and geothermal research*, **156**(3-4): 315-331, https://doi.org/10.1016/j.jvolgeores.2006.03.006.

Smith I E M, Stewart R B, Price R C et al. 2010. Are arc-type rocks the products of magma crystallisation? Observations from a simple oceanic arc volcano: Raoul Island, Kermadec arc, SW pacific. *Journal of Volcanology and Geothermal Research*, **190**(1-2): 219-234, https://doi.org/10.1016/j.jvolgeores.2009.05.006.

Smith I E M, Worthington T J, Price R C et al. 2006. Petrogenesis of dacite in an oceanic subduction environment: Raoul Island, Kermadec arc. *Journal of volcanology and geothermal research*, **156**(3-4): 252-265, https://doi.org/10.1016/j.jvolgeores.2006.03.003.

Spandler C, Pirard C. 2013. Element recycling from subducting slabs to arc crust: a review. *Lithos*, **170-171**: 208-223, https://doi.org/10.1016/j.lithos.2013.02.016.

Stern R J. 2002. Subduction zones. *Reviews of Geophysics*, **40**(4): 3-1-3-38, https://doi.org/10.1029/2001rg000108.

Sutherland R, Hollis C. 2001. Cretaceous demise of the Moa plate and strike-slip motion at the Gondwana margin. *Geology*, **29**(3): 279-282, https://doi.org/10.1130/0091-7613(2001)029<0279:cdotmp>2.0.co;2.

Syracuse E M, van Keken P E, Abers G A. 2010. The global range of subduction zone thermal models. *Physics of the Earth and Planetary Interiors*, **183**(1-2): 73-90, https://doi.org/10.1016/j.pepi.2010.02.004.

Tian L Y, Castillo P R, Hilton D R et al. 2011. Major and trace element and Sr-Nd isotope signatures of the northern Lau basin lavas: implications for the composition and dynamics of the back-arc basin mantle. *Journal of*

Geophysical Research, **116**(B11): B11201, https://doi.org/10.1029/2011JB008791.

Timm C, Bassett D, Graham I J et al. 2013. Louisville seamount subduction and its implication on mantle flow beneath the central Tonga-Kermadec arc. *Nature Communications*, **4**: 1 720, https://doi.org/10.1038/ncomms2702.

Timm C, Davy B, Haase K et al. 2014. Subduction of the oceanic Hikurangi plateau and its impact on the Kermadec arc. *Nature Communications*, **5**: 4 923, https://doi.org/10.1038/ncomms5923.

Timm C, Graham I J, de Ronde C E J et al. 2011. Geochemical evolution of Monowai volcanic center: new insights into the northern Kermadec arc subduction system, SW Pacific. *Geochemistry*, *Geophysics*, *Geosystems*, **12**: Q0AF01, https://doi.org/10.1029/2011gc003654.

Timm C, Leybourne M I, Hoernle K et al. 2016. Trench-perpendicular geochemical variation between two adjacent Kermadec arc volcanoes Rumble II east and west: the role of the subducted Hikurangi plateau in element recycling in arc magmas. *Journal of Petrology*, **57**(7): 1 335-1 360, https://doi.org/10.1093/petrology/egw042.

Turner S, Bourdon B, Hawkesworth C et al. 2000. ^{226}Ra-^{230}Th evidence for multiple dehydration events, rapid melt ascent and the time scales of differentiation beneath the Tonga-Kermadec island arc. *Earth and Planetary Science Letters*, **179**(3-4): 581-593, https://doi.org/10.1016/S0012-821X(00)00141-2.

Turner S, Caulfield J, Rushmer T et al. 2012. Magma evolution in the primitive, intra-oceanic Tonga arc: rapid petrogenesis of dacites at Fonualei volcano. *Journal of Petrology*, **53**(6): 1 231-1 253, https://doi.org/10.1093/petrology/egs005.

Turner S, Handler M, Bindeman I et al. 2009. New insights into the origin of O-Hf-Os isotope signatures in arc lavas from Tonga-Kermadec. *Chemical Geology*, **266**(3-4): 187-193, https://doi.org/10.1016/j.chemgeo.2009.05.027.

Turner S, Hawkesworth C, Rogers N et al. 1997. ^{238}U-^{230}Th disequilibria, magma petrogenesis, and flux rates beneath the depleted Tonga-Kermadec island arc. *Geochimica et Cosmochimica Acta*, **61**(22): 4 855-4 884, https://doi.org/10.1016/s0016-7037(97)00281-0.

Turner S, Hawkesworth C. 1997. Constraints on flux rates and mantle dynamics beneath island arcs from Tonga-Kermadec lava geochemistry. *Nature*, **389**(6651): 568-573, https://doi.org/10.1038/39257.

Turner S, Hawkesworth C. 1998. Using geochemistry to map mantle flow beneath the Lau Basin. *Geology*, **26**(11): 1 019-1 022, https://doi.org/10.1130/0091-7613(1998)026<1019:Ugtmmf>2.3.Co;2.

van Keken P E, Hacker B R, Syracuse E M et al. 2011. Subduction factory: 4. Depth-dependent flux of H_2O from subducting slabs worldwide. *Journal of Geophysical Research*, **116**(B1): B01401, https://doi.org/10.1029/2010JB007922.

van Keken P E, Kiefer B, Peacock S M. 2002. High-resolution models of subduction zones: implications for mineral dehydration reactions and the transport of water into the deep mantle. *Geochemistry*, *Geophysics*, *Geosystems*, **3**(10): 1-20, https://doi.org/10.1029/2001GC000256.

Wendt J I, Regelous M, Collerson K D et al. 1997. Evidence for a contribution from two mantle plumes to island-arc lavas from northern Tonga. *Geology*, **25**(7): 611-614, https://doi.org/10.1130/0091-7613(1997)025<0611:efacft>2.3.co;2.

Woodhead J, Eggins S, Gamble J. 1993. High field strength and transition element systematics in island arc and back-arc basin basalts: evidence for multi-phase melt extraction and a depleted mantle wedge. *Earth and Planetary Science Letters*, **114**(4): 491-504, https://doi.org/10.1016/0012-821X(93)90078-N.

Wyllie P J. 1979. Magmas and volatile components. *American Mineralogist*, **64**(5-6): 469-500.

Zellmer G F, Edmonds M, Straub S M. 2015. Volatiles in subduction zone magmatism. *Geological Society*, *London*, *Special Publications*, **410**(1): 1-17, https://doi.org/10.1144/sp410.13.

Zhang G L, Smith-Duque C, Tang S H et al. 2012. Geochemistry of basalts from IODP Site U1365: implications for magmatism and mantle source signatures of the mid-cretaceous osbourn trough. *Lithos*, **144-145**: 73-87, https://doi.org/10.1016/j.lithos.2012.04.014.

Zhang G L, Smith-Duque C. 2014. Seafloor basalt alteration and chemical change in the ultra thinly sedimented south pacific. *Geochemistry*, *Geophysics*, *Geosystems*, **15**(7): 3 066-3 080, https://doi.org/10.1002/2013GC005141.

Zhang G, Li C. 2016. Interactions of the greater Ontong Java mantle plume component with the Osbourn Trough. *Scientific Reports*, **6**: 37 561, https://doi.org/10.1038/srep37561.